A Mechanical Descriptor of Instability in Human Locomotion: Experimental Findings in Control Subjects and People with Transfemoral Amputation

Nahime Al Abiad, Helene Pillet, Bruno Watier

A Mechanical Descriptor of Instability in Human Locomotion: Experimental Findings in Control Subjects and People with Transfemoral Amputation

Nahime Al Abiad [1,*], Hélène Pillet [2] and Bruno Watier [1]

[1] Laboratoire d'Analyse et d'Architecture des Systèmes (LAAS-CNRS), Université de Toulouse, CNRS, UPS, 31031 Toulouse, France; bruno.watier@univ-tlse3.fr

[2] Arts et Métiers/Institut de Biomécanique Humaine Georges Charpak, 151 boulevard de l'Hôpital, 75013 Paris, France; helene.pillet@ensam.eu

[*] Correspondence: naimamohabiad@gmail.com

Featured Application: This study could be useful when comparing the balance of standard and instrumented walking (e.g., elderly, prosthesis, exoskeleton) on uneven terrains. Moreover, it can be helpful in the field of motion generation of humanoid robotics.

Abstract: While multiple criteria to quantify gait instability exist, some limitations hinder their computation during realistic walking conditions. A descriptor, computed as the distance between the center of mass of the body and the minimal moment axis ($d_{COM-\Delta}$), has been proposed recently. This present study aims at characterizing the behavior of the mentioned descriptor in a population at a higher risk of falls. Five individuals with transfemoral amputation and 14 healthy individuals were involved in an experiment composed of motion capture and force plates acquisition during overground walking at a self-selected speed. For both groups of participants, the profile of $d_{COM-\Delta}$ was analyzed and descriptive parameters were calculated. The plot of $d_{COM-\Delta}$ was different between groups and different relative to the leading limb considered (prosthetic or contralateral). All descriptive parameters calculated, except one, were statistically different between groups. As a conclusion, amputees seem to be able to limit the average of $d_{COM-\Delta}$ in spite of a different evolution pattern. This is consistent with the ability of the subjects to maintain their dynamic balance. However, the extracted parameters showed the significant asymmetry of the gait profile between prosthetic and contralateral stances and highlighted the potential sources of imbalance.

1. Introduction

Behind humans locomotion lies a complex musculoskeletal system responsible simultaneously for the balance and displacement. For decades, it has been the focus of researchers to find some criteria upon which this system relies. Existing criteria are either based on static or dynamic conditions. For static situations, the common condition used is that the vertical projection of the center of mass (COM) falls within the convex hull of contact points between feet and ground, also called the support polygon [1]. However, it has been proved that this condition is invalid during dynamic conditions such as walking [2]. A widely used concept in dynamic situations is the zero moment point (ZMP), also called the center of pressure (COP). The criteria state that to achieve minimum instability, the ZMP should fall within the support polygon during the motion [3]. Nevertheless, the concept of ZMP has been the subject of various polemics among scientists. First of all, the ZMP cannot exist outside the support polygon and, therefore, cannot be predictive of the risk

of falling [4]. Second, the support polygon and ZMP are not adapted to multi-contact locomotion or on uneven ground. Thus, a generalized stability criterion is yet to be established [5].

Several attempts have been done to generalize the concept of ZMP and predict falling risks. In this perspective, Hof et al. [6] have defined a point called the extrapolated center of mass (XCOM). It considers the position of the COM together with its velocity and should also fall within the support polygon to achieve a stable gait. However, some cases exist where this point is outside the support polygon and no falling is observed. When considering gait on uneven terrain, a new difficulty appears regarding the definition of the support polygon. Caron et al. have described a 3-dimensional convex hull built from two non-coplanar real support areas. The gait is said to be in balance if the ZMP falls inside a certain projection of this 3D convex hull [7]. Similarly, Sardain et al. have worked on defining a virtual surface and a virtual ZMP [8]. In contrast to the above-mentioned approaches which focus on monitoring a point with respect to the support polygon, Popovic et al. have approached the subject by studying the angular momentum during gait. They assumed that the minimization of the angular momentum at the COM is an aim of the nervous system [9]. Finally, Maus et al. have modeled gait with a virtual pendulum model and have defined a virtual pivot point (VPP) where the resultant ground reaction forces intersect [10]. Additional research has been done by Gruben et al. to interpret whether it is an objective of the nervous system to make forces intersect at the VPP [11].

Recently, Bailly et al. proposed a new mechanical descriptor [5] based on an approach related to ground reaction forces and moments (GRF&M), and COM position. GRF&M can be represented by an external contact wrench (ECW). The central axis of the ECW, also called the minimum moment axis (MMA), is the axis along which the Euclidean norm of the moment is minimal and collinear to the resultant force [12]. The distance between the COM and the MMA was suggested as a locomotion descriptor. The effectiveness of this descriptor lies in its ability to describe the derivate of the angular momentum at the COM throughout the phases of the gait cycle, and in its capacity to be computed for generalized locomotion (uneven surfaces or multi contacts). Considering the derivate of the angular momentum at COM, as mentioned above, Popovic et al. concluded that the angular momentum is highly regulated by the central nervous system throughout a movement cycle [9]. According to Newton's 2nd law, the derivate of this angular momentum is equal to the moment at the COM. Briefly speaking, as the distance between the COM and the MMA decreases, the variation of angular momentum at the COM decreases and vice versa. Several experiments involving multi-contact locomotion were previewed in the paper of Bailly et al. They conclude that the distance increases as the walking terrain increases in difficulty, implying that this distance may be used to quantify instability and risks of falling during gait [5].

Many questions about the distance's evolution over the gait cycle, the characteristics of the distance that can signify the imbalance and, the distance's ability to differentiate between normal and abnormal gaits remain to be answered. To bring some elements of an answer, the concept must be tested in challenging conditions. Walking with a prosthesis can be considered so as it has been previously used in the literature to test several indicators of balance [13].

Thus, this present study aims to evaluate and characterize the behavior of the aforementioned descriptor in a population with a higher risk of falls [14]. The hypothesis is that the distance between the COM and the MMA calculated on amputees will be able to signify instabilities. Thus, this study should provide reference data for this original descriptor that could be used to monitor the evolution of gait.

2. Materials and Methods

2.1. Participants

Five people with unilateral transfemoral amputation (age 44 ± 14 years, height 1.8 ± 0.1 m, body mass 73 ± 17 kg) and 14 healthy subjects (age 25.6 ± 5.8 years, height 1.77 ± 0.35 m, body mass 73 ± 8 kg) volunteered for this study. Table 1 shows the characteristics of the participants with transfemoral amputation and the number of trials they performed. The healthy subjects had no prior or existing

injury or neurological disorder affecting the gait. People with amputation were able to walk without additional assistive devices and were free of musculoskeletal disorders on the residual side. The data used in the study were taken from two laboratories. For healthy subjects, the data were collected from Laboratoire d'Analyses et d'Architectures des Systèmes du CNRS (Toulouse, France) database, and for amputees, they were obtained from Institut de Biomécanique Humaine Georges Charpak des Arts et Métiers (Paris, France) database. Each participant signed an informed consent after formal approval of the protocol by the ethics evaluation committee (Comité de Protection des Personnes, CPP NX06036).

Table 1. Characteristics of participants with transfemoral amputation (BMI: Body Mass Index).

N°	N° of Trials	Gender	Age (y)	Height (m)	Weight (Kg)	BMI (Kg/m²)	Amputation Delay (Years)	Foot Type	Knee Type
A1	1	M	54	1.8	85	25.9	7	1C40® (Ottobock)	CLEG 3 ® (Ottobock)
A2	5	F	49	1.7	53	19.4	25	Elation ® (Ossur)	Total Knee ® (Ossur)ossur
A3	2	F	26	1.7	65	23.9	2,5	Elation ® (Ossur)	RheoKnee ® (Ossur)
A4	2	M	32	1.8	95	29.3	7	Proflex ® (Ossur)	RheoKnee XC ® (Ossur)
A5	1	M	58	1.8	68	21.9	31	Variflex	Mauch SNS
Mean	-	-	44	1.8	73	24	15	-	-
SD	-	-	14	0.1	17	4	13	-	-

2.2. Experimental Protocol

Each participant had to execute a simple spontaneous-speed walking task in a gait analysis laboratory, on force plates measuring the external wrenches (forces and moments) at 2 kHz. The configuration and size of the force plates in each laboratory allowed to record three steps per trial. A set of 47 passive reflective markers were used following the protocol described by Maldonado et al. [15] (Figure 1). An optoelectronic system (Vicon, Oxford, UK) was used to capture full-body static and kinematic data at 200 Hz. The number of correct trials performed by subjects with amputation is given in Table 1 while the number of correct trials performed by healthy subjects is 3.
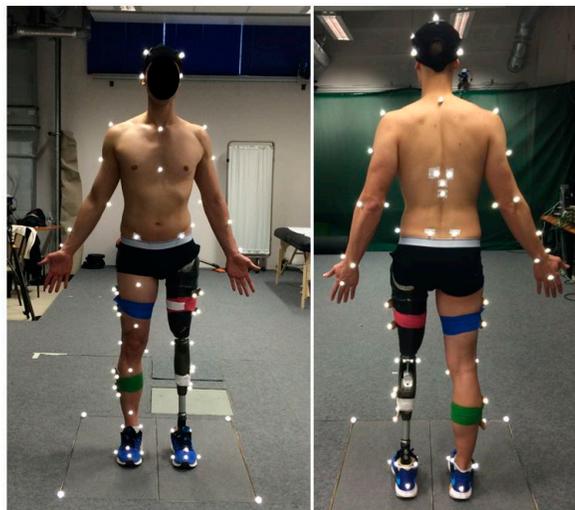

Figure 1. Reflective markers placed on a subject with transfemoral amputation; 47 markers were used in the present study according to the protocol described by Maldonado et al. [15].

2.3. Center of Mass Computation

For healthy individuals and sound body segments of people with amputation, the segments' masses and COM positions were obtained in their local frame from anthropometric tables [16].

For the prosthetic limb, the computation of COM was performed as follows: the mass and the COM position of the residual limb were obtained by the geometrical modeling of the residual limb using the method described by Pillet et al. [17]. The mass of the socket, estimated to be 0.8 kg, was systematically added. A concentrated mass was used to model the prosthetic leg and the prosthetic foot. The mass of the prosthetic leg encompasses the prosthetic knee's mass taken from manufacture notices and a 0.3 kg corresponding to the prosthetic shank and connectors. The mass of the prosthetic foot is composed of the prosthetic foot's mass taken from the manufacturer's notice. Due to the inability of people with amputation to walk barefooted, the mass of the shoes was added to each foot. The COM's positions were estimated from the markers placed on the prosthetic lower limb at the knee, ankle and midfoot. Finally, the trajectory of the reflective markers placed on the subject's anatomical landmarks was filtered with a 4th order Butterworth low-pass with a cutoff frequency fixed at 15 Hz and used to construct local frames at each instant to compute the instantaneous position of body segments' center of masses. The global COM instantaneous position could then be inferred.

2.4. Minimum Moment Axis Computation

Ground reaction forces and moments were measured by force plates and filtered using a 4th order, zero phase-shift, low-pass Butterworth with a 15 Hz cut-off frequency.

At any point A, external mechanical actions applied on the foot can be represented by a force $\boldsymbol{F}$ and a moment $\boldsymbol{M_A}$. $\boldsymbol{F}$ and $\boldsymbol{M_A}$ define a moment field that can be expressed at any point B as:

$$\boldsymbol{M_B} = \boldsymbol{M_A} + \boldsymbol{F} \times \boldsymbol{P_{(A,B)}} \tag{1}$$

where $\boldsymbol{P_{(A,B)}}$ is the position of B with respect to A.

There exists one axis Δ such that, at each point of this axis, the moment is collinear to $\boldsymbol{F}$ [18]. This axis is called the central axis of the external contact wrench. We can demonstrate that the moment in space is minimum along this axis. Assume that point $Q \in \Delta$. Δ is computed as in [5]:

$$\forall B \ in \ space, \forall Q \ \in \Delta, \boldsymbol{P_{(B,Q)}} = \frac{\boldsymbol{F} \times \boldsymbol{M_B}}{\|\boldsymbol{F}\|^2} + \lambda \boldsymbol{F}, \qquad \lambda \epsilon \mathbb{R} \tag{2}$$

If we now assume that B is the COM:

$$\forall Q \ \in \Delta, \qquad \boldsymbol{P_{(COM,Q)}} = \frac{\boldsymbol{F} \times \boldsymbol{M_{COM}}}{\|\boldsymbol{F}\|^2} + \lambda \boldsymbol{F}, \qquad \lambda \epsilon \mathbb{R} \tag{3}$$

When $\lambda = 0$, Q is the orthogonal projection of the COM onto Δ and the distance $\|\boldsymbol{P_{(COM,Q)}}\|$ is the minimal distance between Δ and the COM. The vector $\boldsymbol{P_{(COM,Q)}}$ will be called $\boldsymbol{d_{COM-\Delta}}$ hereafter:

$$\boldsymbol{d_{COM-\Delta}} = \frac{\boldsymbol{F} \times \boldsymbol{M_{COM}}}{\|\boldsymbol{F}\|^2} \tag{4}$$

From Equation (4), we compute the Euclidian norm of the distance from COM position and force platform data:

$$\|\boldsymbol{d_{COM-\Delta}}\| = \frac{\|\boldsymbol{F} \times \boldsymbol{M_{COM}}\|}{\|\boldsymbol{F}\|^2} \tag{5}$$

Interestingly, it can be noted that this distance can also be linked to the angular momentum at the COM by considering the relation: $\dot{\boldsymbol{h}}_{COM} = \boldsymbol{M_{COM}}$ where $\dot{\boldsymbol{h}}_{COM}$ is the derivative of the angular momentum. Thus:

$$\|\boldsymbol{d_{COM-\Delta}}\| = \frac{\|\dot{\boldsymbol{h}}_{COM}\| \cdot |sin \theta|}{\|\boldsymbol{F}\|} \tag{6}$$

With θ is the angle between $\boldsymbol{F}$ and $\dot{\boldsymbol{h}}_{COM}$.

We project $\boldsymbol{d}_{COM-\Delta}$ in Equation (4) on the subject's anterior-posterior axis, medial-lateral axis, and vertical axis:

$$\begin{bmatrix} d_{ML} \\ d_{AP} \\ d_V \end{bmatrix} = \frac{1}{\|\boldsymbol{F}\|^2} \begin{bmatrix} F_{AP} \times M_V - F_V \times M_{AP} \\ F_V \times M_{ML} - F_{ML} \times M_V \\ F_{ML} \times M_{AP} - F_{AP} \times M_{ML} \end{bmatrix} \tag{7}$$

where d_{ML}, d_{AP}, d_V respectively refer to the medio-lateral, anterior-posterior and vertical component of $\boldsymbol{d}_{COM-\Delta}$.

2.5. Time Segmentation

For asymptomatic people, the descriptive parameters can be considered as symmetrical. Therefore, the analysis of one limb per trial is enough. On the contrary, in the case of highly asymmetrical patterns found with people with amputation, the cycle of each limb must be isolated and analyzed separately.

Considering the force plates configuration, the usual period lying from the heel strike of one limb to the consecutive heel strike of the same limb could not be isolated. To compare individual patterns, a procedure of segmentation is proposed in Figure 2.
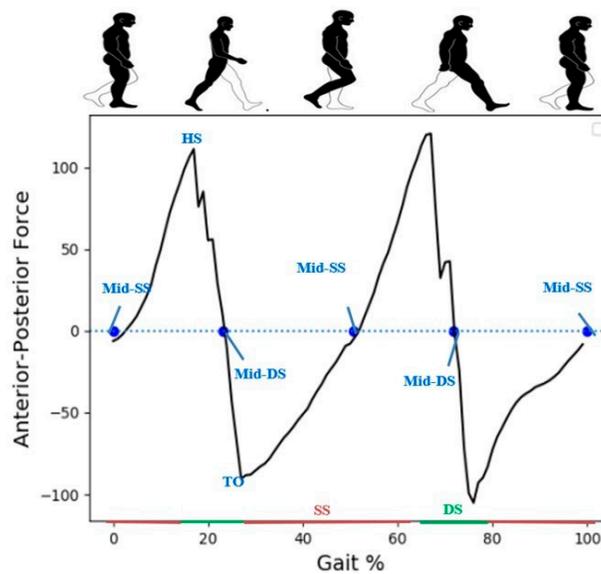

Figure 2. Healthy subject anterior-posterior force segmentation (SS: Single Stance, DS: Double Stance, TO: Toe off, HS: Heel strike).

The data were cropped considering the zeros of the anteroposterior force. The anteroposterior force becomes null at mid-stance or mid-swing, and mid-double stance. The analyzed data included 5 zeros of the anteroposterior force. After cropping, time was normalized between 0% and 100% corresponding to the first and last zeros.

2.6. Descriptive Parameters

To describe the distance pattern, several parameters from the individual curve were extracted. The parameters were:

- Gait speed estimated as the average of the derivative of the COM trajectory along the anterior-posterior axis.
- $\overline{d_{COM-\Delta}}$: The average distance over the gait cycle.

$$\overline{d_{COM-\Delta}} = \sum_{i \in n} \frac{d_{COM-\Delta}^{i}}{n} \tag{8}$$

where $d_{COM-\Delta}^{i}$ is the ith sample recorded within the gait cycle, and n is the total number of samples collected.

- $\max(d_{COM-\Delta})$: Local maximum distance.

$$\max(d_{COM-\Delta}) = \max_{i \in N} d_{COM-\Delta}^{i} \tag{9}$$

where N = {j, …, k}. j and k represent the start and end of the interval where the local maximum is sought.

- *Drop* $(d_{COM-\Delta})$: Variation of distance's amplitude at heel strike. In other words, it is the difference between local maximum and minimum around the instant of heel strike.

$$Drop\ (d_{COM-\Delta)} = \max_{i \in N} d_{COM-\Delta}^{i} - \min_{i \in N} d_{COM-\Delta}^{i} \tag{10}$$

- The anterior-posterior distance at heel strike and toe off.

2.7. Statistics

All the parameters were computed for each trial, and then the average and standard deviation of all healthy subjects were obtained. For amputees, due to the difference in characteristics (prosthesis, step length), the parameters were computed for each subject for both prosthetic and sound limb events. A non-parametric two-sample Mann–Whitney test was done for each extracted parameter from the distance curve to compare both groups of subjects considering successively the prosthetic and the sound limb. A *p*-value of 0.05 was defined as the level of statistical significance.

3. Results

The profiles of the $d_{COM-\Delta}$ and d_{AP} according to time are shown in Figure 3A on average for healthy subjects and in Figure 3B for one typical subject with amputation. Note that the subject with amputation starts walking on the force platform with his prosthetic limb.

Table 2 shows the values of the descriptive parameters listed above. The absolute value of d_{AP} and $d_{COM-\Delta}$ are shown in Figure 4.

Table 2. Calculated parameters among amputees (A1, A2, A3, and A4) and healthy subjects. HS: Heel Strike, TO: Toe Off, SL: Sound limb, PL: Prosthetic limb.

| Parameter	A1	A2	A3	A4	A5	Healthy (n = 14)	*p*-Value
$\overline{d_{COM-\Delta}}$	47	41 ± 2	38 ± 1	45 ± 3	33	37 ± 4.5	>0.05
max$(d_{COM-\Delta})$ before HS of SL (mm)	124	111 ± 5	108 ± 7	135 ± 3	96	79 ± 10	<0.05
max$(d_{COM-\Delta})$ before HS of PL (mm)	54	56 ± 3	62 ± 8	53 ± 0.	30		<0.05
Drop $d_{COM-\Delta}$ at HS of SL (mm)	93	106 ± 5	92 ± 8	129 ± 9	84	68 ± 11	<0.05
Drop $d_{COM-\Delta}$ at HS of PL (mm)	41	38 ± 18	50 ± 1	43 ± 2	24		<0.05
d_{AP} at HS of SL (mm)	111	107 ± 5	101 ± 5	124 ± 6	90	76 ± 10	<0.05
d_{AP} at HS of PL (mm)	52	53 ± 7	62 ± 9	53 ± 0.	29		<0.05
d_{AP} at TO of SL (mm)	40	55 ± 3	37 ± 7	57 ± 1	43	19 ± 6	<0.05
d_{AP} at TO of PL (mm)	1	6 ± 9	7 ± 3	−1 ± 0.	19		<0.05
Gait speed (m/s)	1.13	1.27 ± 0.0	1.14 ± 0.0	1.3 ± 0.1	1.33	1 ± 0.2	<0.05

(**a**)

(**b**)
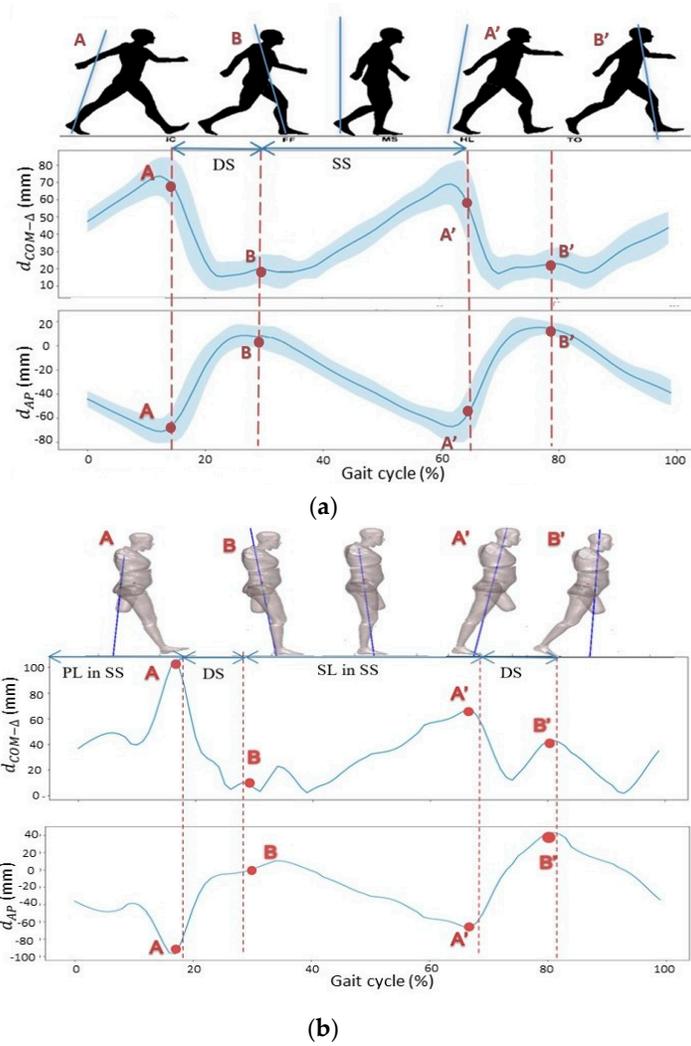
Figure 3. The plot of the distance between minimal moment axis and center of mass (COM) ($d_{COM-\Delta}$), and the anterior-posterior component (d_{AP}), relative to the gait cycle, for the average of healthy subjects (**a**) and an amputee subject (**b**). (A: First Heel Strike, B: First Toe Off, A': second Heel Strike, B': second Toe Off, DS: double stance, SS: single stance, PL: prosthetic limb, SL: Sound Limb).
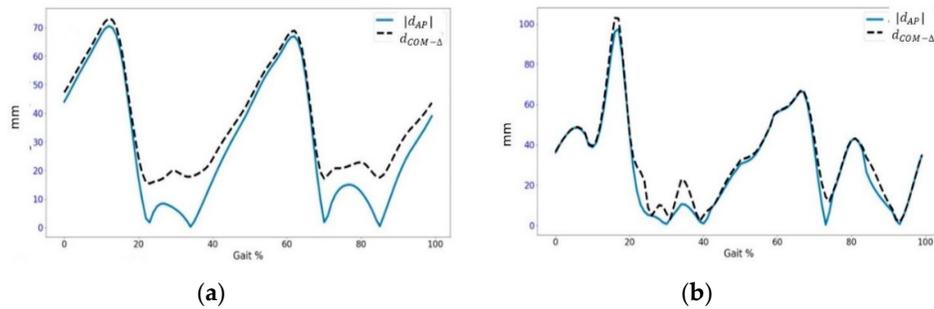

(**a**)   (**b**)

Figure 4. Evolution of the norm of the distance between minimal moment axis and COM ($d_{COM-\Delta}$) dashed line and the absolute value of the anterior-posterior component (d_{AP}) full-line, during the gait cycle, for the average of healthy subjects (**a**) and one person with amputation (**b**).

4. Discussion

To analyze the mechanism behind how humans fall during dynamic activities, it is relevant to find a way to quantify dynamic instability. The goal of this study is to determine whether the descriptor mentioned above may be a potential measure of dynamic instability.

To address the matter, results in Table 2 show that the aforementioned descriptive parameters calculated on healthy subjects are statistically different than those calculated on subjects with amputation. The only exception is the average distance. Indeed, the average distance for people with amputation is close to the average distance of healthy subjects. This means that (1) if the average distance is a measure of instability, then the instability in amputee's gait is similar to that in healthy subject's gait; (2) however, other extracted parameters from distance curve were able to differentiate between subjects with amputation gait and healthy subject's gait.

Considering healthy subjects, the profile of the distance is similar to the one found in the paper of Bailly et al. (Figure 3). The MMA is farthest away behind the subject's COM at the end of the swing phase (Figure 3: point A). At this time, the MMA is inclined toward the subject's COM. This contributes to a decrease in the maximum distance. Regarding the anterior-posterior distance, its profile is similar to the profile of the dimensionless spin along the mediolateral axis of the subject obtained in the paper of Popovic et al. During the swing phase, the subject's angular momentum like the anterior-posterior distance is negative and its magnitude is increasing. This gives the subject a tendency to rotate forward which is useful to the forward progression of the body. At heel strike, we can notice a drop in the distance. Thus, the MMA moves toward the COM and crosses it. It is now in front of the body (Figure 3: point B). However, the anterior-posterior distance at this point is much lower than at the end of the swing phase. Similarly, the positive angular momentum is much lower than the negative angular momentum through the gait cycle. This means that, while walking, the tendency to fall forward is much higher than the tendency to fall backward. One can note that the MMA is always inclined forward when d_{AP} is negative and conversely inclined backward when d_{AP} is positive.

Despite using different prostheses, amputees showed similar characteristics. The pattern of the distance is asymmetrical. The MMA is further behind the body when the prosthetic limb is in the stance phase than when it is in the swing phase. This can be related to the limited inclination of the axis towards the COM, which may result in more instability and less comfort when the stance is on the prosthesis. This agrees with previous studies that state that the sound limb has higher dynamic stability [19]. The event heel strike also ensures a drop in the distance; however, the sound limb stance results in a much higher drop than the prosthetic one. The MMA is now in front of the body. It is further in front after the event toe off of the sound limb than the event toe off of the prosthetic limb. Therefore, as long as the sound limb is on the ground supporting the body, it can correct any instability [19,20]. The sound limb is much more active in amputee gait, especially in producing the stabilizing and compensatory effects.

The parameters that play a significant role in the distance are the GRF&M (anterior-posterior force, vertical force) and the COM position. The plot of the 3D distance and the anterior-posterior distance in Figure 4 shows that due to the prominent value of F_V the 3D distance can be approximated to be:

$$d_{com-\Delta} \approx d_{AP} \approx \frac{F_V . M_{ML}}{\|F\|^2}, \tag{11}$$

$$M_{ML} = (r_y F_V - r_z F_{AP}), \tag{12}$$

Castro et al. [21] showed that the ground reaction forces produced by the prosthetic side are less than those produced by the sound side. Most importantly, the prosthetic side is not able to produce an adequate amount of push and break (F_{AP}). This means that the subject's COM is not able to gain the normal acceleration and deceleration when the prosthetic limb is in stance phase. This is consistent with the lower MMA inclination. The height of COM r_z is also lower during prosthetic foot stance phase [22]. The term r_y is the foot forward placement (FFP). It is the distance between the COM and the leading foot as defined by Hak et al. [23]. They proved that the asymmetry in

amputees' step length is due to the asymmetry in the FFP. It has been mentioned by previous studies that amputees' step asymmetry helps in preserving stability.

The above-mentioned parameters, shown schematically in Figure 5: the FFP, the COM height, the external forces and moments are all wrapped up in one significant parameter: the distance. The control of any mentioned parameter contributes to the control of the distance. Finally, the distance describes the angular momentum because the external moment is equal to the derivate of the angular momentum Equation (6). Our results are consistent with the ones of Popovic et al. who have proposed that the healthy subjects control the variation of the angular momentum [9].

Surprisingly, the walking speed of subjects with amputation was higher than the speed of healthy subjects. This result can be attributed to the different laboratory setup and arrangement of force plates. However, this difference is not significant and its impact on the distance can be neglected. When the speed effect was studied by Bailly et al. a much higher speed difference between groups was taken into consideration [5].

The classic limitations of studies involving people with amputation include low subject numbers, heterogeneity of levels of amputation, of prosthetic types and walking speeds. To generalize the aforementioned conclusions, an extensive study must be conducted. Another limitation found when comparing healthy to amputee subjects is related to walking conditions i.e., barefoot vs. with shoes. Because the prosthesis alignment is always performed with shoes on, people with amputations are generally not able to walk barefooted which is the classical condition of walking in studies involving healthy subjects. In the present study, the cohort of healthy subjects serves as a reference and the variability due to the use of different types of shoes would have hindered the homogeneity of the results. Thus, the compromise chosen in the study was to keep the walking condition best suited to the group of subjects considered.
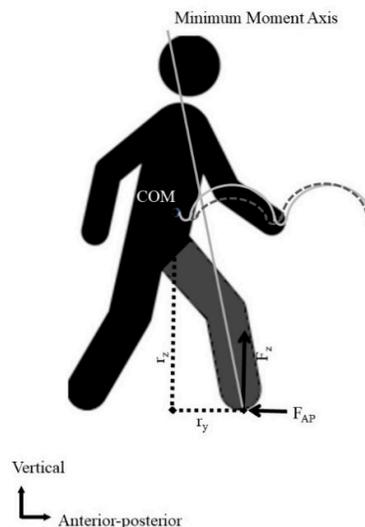

Figure 5. Representation in the sagittal plane of the mechanical parameters involved in the computation of $d_{COM-\Delta}$. r_z: height of COM, r_y: the anterior-posterior distance between COM and the intersection of the minimal moment axis Δ with the ground. The trajectories of COM in the sagittal plane are illustrated as a dashed line (amputee) and full line (healthy subject).

5. Conclusions

In this study, we assessed the ability of a mechanical descriptor on quantifying dynamic instability during gait. The distance was computed for healthy subjects and people with transfemoral amputation. Some parameters and characteristics that were extracted from the distance vs. time curves were able to differentiate significantly between the studied groups. Results show that the distance can be used to highlight some instability features, and that it is probably controlled by the nervous system to maintain stability.

Conflicts of Interest: The authors declare no conflict of interest.

References

1. Winter, D.A. Human balance and posture control during standing and walking. *Gait Posture* **1995**, *3*, 193–214, doi:10.1016/0966-6362(96)82849-9.
2. Patton, J.L.; Pai, Y.C.; Lee, W.A. Evaluation of a model that determines the stability limits of dynamic balance. *Gait Posture* **1999**, *9*, 38–49, doi:10.1016/s0966-6362(98)00037-x.
3. Vukobratovic, M.; Borovac, B. Zero moment point—Thirty five years of its life. *Int. J. Hum. Robot.* **2004**, *1*, 157–173, doi:10.1142/S0219843604000083.
4. Kajita, S.; Hirukawa, H.; Harada, K.; Yokoi, K. *Introduction à la Commande des Robots Humanoïdes*; Springer Paris, France, 2009, ISBN 978-2-287-87715-5.
5. Bailly, F.; Carpentier, J.; Pinet, B.; Souères, P.; Watier, B. A Mechanical Descriptor of Human Locomotion and its Application to Multi-Contact Walking in Humanoids. In Proceedings of the IEEE RAS and EMBS International Conference on Biomedical Robotics and Biomechatronics, Enschede, The Netherlands, 26–29 August 2018; pp. 350–356, doi:10.1109/BIOROB.2018.8488125.
6. Hof, A.L.; Gazendam, M.G.J.; Sinke, W.E. The condition for dynamic stability. *J. Biomech.* **2005**, *38*, 1–8, doi:10.1016/j.jbiomech.2004.03.025.
7. Caron, S.; Pham, Q.C.; Nakamura, Y. ZMP Support Areas for Multicontact Mobility under Frictional Constraints. *IEEE Trans. Robot.* **2017**, *33*, 67–80, doi:10.1109/TRO.2016.2623338.
8. Sardain, P.; Bessonnet, G. Forces acting on a biped robot. Center of pressure-Zero moment point. *IEEE Trans. Syst. Man Cybern. Part A Syst. Hum.* **2004**, *34*, 630–637, doi:10.1109/TSMCA.2004.832811.
9. Popovic, M.; Hofmann, A.; Herr, H. Angular momentum regulation during human walking: Biomechanics and control. In Proceedings of the IEEE International Conference on Robotics and Automation, 2004. Proceedings. ICRA '04, New Orleans, LA, USA, 26 April–1 May 2004; doi:10.1109/robot.2004.1307421.
10. Maus, H.M.; Lipfert, S.W.; Gross, M.; Rummel, J.; Seyfarth, A. Upright human gait did not provide a major mechanical challenge for our ancestors. *Nat. Commun.* **2010**, *1*, 1–6., doi:10.1038/ncomms1073.
11. Gruben, K.G.; Boehm, W.L. Force direction pattern stabilizes sagittal plane mechanics of human walking. *Hum. Mov. Sci.* **2012**, *31*, 649–659, doi:10.1016/j.humov.2011.07.006.
12. Gallardo-Alvarado, J. *Kinematic Analysis of Parallel Manipulators by Algebraic Screw Theory*; Springer International Publishing, 2016; ISBN 9783319311265.
13. Hof, A.L.; van Bockel, R.M.; Schoppen, T.; Postema, K. Control of lateral balance in walking. Experimental findings in normal subjects and above-knee amputees. *Gait Posture* **2007**, *25*, 250–258, doi:10.1016/j.gaitpost.2006.04.013.

14. Miller, W.C.; Speechley, M.; Deathe, B. The prevalence and risk factors of falling and fear of falling among lower extremity amputees. *Arch. Phys. Med. Rehabil.* **2001**, *82*, 1031–1037, doi:10.1053/apmr.2001.24295.

15. Maldonado, G.; Souères, P.; Watier, B. *Whole-Body Musculo-Skeletal Model V1*; [Technical Report] Rapport LAAS n° 18233, LAAS-CNRS. hal-01841355; Université de Toulouse 3 Paul Sabatier: Toulouse, France, 2018.

16. Dumas, R.; Chèze, L.; Verriest, J.P. Adjustments to McConville et al. and Young et al. body segment inertial parameters. *J. Biomech.* **2007**, *40*, 543–553, doi:10.1016/j.jbiomech.2006.02.013.

17. Pillet, H.; Bonnet, X.; Lavaste, F.; Skalli, W. Evaluation of force plate-less estimation of the trajectory of the centre of pressure during gait. Comparison of two anthropometric models. *Gait Posture* **2010**, *31*, 147–152, doi:10.1016/j.gaitpost.2009.09.014.

18. Shimba, T. An estimation of center of gravity from force platform data. *J. Biomech.* **1984**, *17*, 53–60, doi:10.1016/0021-9290(84)90080-0.

19. Kendell, C.; Lemaire, E.D.; Dudek, N.L.; Kofman, J. Indicators of dynamic stability in transtibial prosthesis users. *Gait Posture* **2010**, *31*, 375–379, doi:10.1016/j.gaitpost.2010.01.003.

20. Mohamed, A.; Sexton, A.; Simonsen, K.; McGibbon, C.A. Development of a mechanistic hypothesis linking compensatory biomechanics and stepping asymmetry during gait of transfemoral amputees. *Appl. Bionics Biomech.* **2019**, *2019*, 4769242, doi:10.1155/2019/4769242.

21. Castro, M.P. de; Soares, D.; Mendes, E.; Machado, L. Plantar pressures and ground reaction forces during walking of individuals with unilateral transfemoral amputation. *PM&R* **2014**, *6*, 698–707.e1, doi:10.1016/j.pmrj.201.

22. Strutzenberger, G.; Alexander, N.; De Asha, A.; Schwameder, H.; Barnett, C.T. Does an inverted pendulum model represent the gait of individuals with unilateral transfemoral amputation while walking over level ground? *Prosthet. Orthot. Int.* **2019**, *43*, 221–226, doi:10.1177/0309364618796847.

23. Hak, L.; van Dieen, J.H.; van der Wurff, P.; Houdijk, H. Stepping Asymmetry Among Individuals with Unilateral Transtibial Limb Loss Might Be Functional in Terms of Gait Stability. *Phys. Ther.* **2014**, *94*(10), 1480-1488, doi: 10.2522/ptj.20130431.